ARTICLE

Electronic Supplementary Information

Rhodamine 6G and 800 intermolecular heteroaggregates embedded in PMMA for Near-Infrared wavelength shifting

Javier Castillo-Seoane, Lola Gonzalez-Garcia†, José M. Obrero-Perez, Francisco J. Aparicio, Ana Borrás, Agustín R. González-Elipe, Ángel Barranco*, Juan R. Sanchez-Valencia*

Table S1. Actual concentration of Rh6G and Rh800 in the PMMA samples using Equation 1.

Sample	C_{Rh6G} [mM]	C_{Rh800} [mM]	Relative concentration of C_{Rh6G}/C_{Rh800}
0-1	0.00	2.26	-
0-2	0.00	6.72	-
0-3	0.00	22.38	-
1-0	2.26	0.00	-
1-1	2.25	2.25	1.00
1-2	2.25	6.72	0.34
1-3	2.24	22.36	0.10
2-0	6.73	0.00	-
2-1	6.72	2.25	2.99
2-2	6.71	6.71	1.00
2-3	6.66	22.32	0.30
3-0	22.40	0.00	-
3-1	22.38	2.24	10.00
3-2	22.33	6.67	3.35
3-3	22.19	22.19	1.00

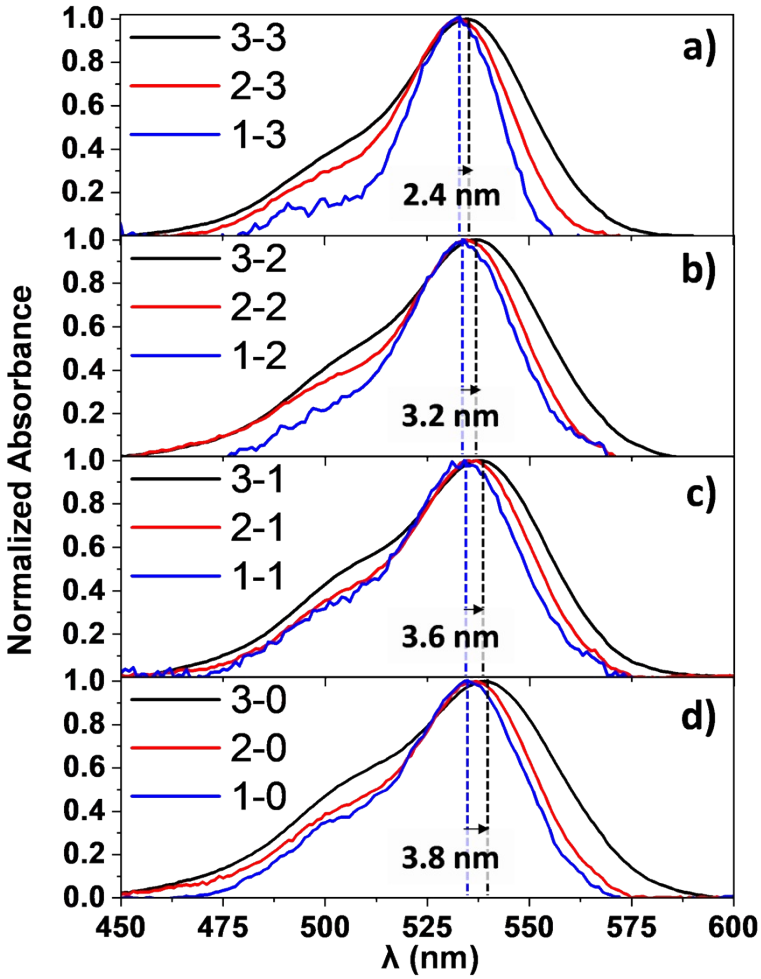

Figure S1. Normalised absorbance spectra (subtracting a horizontal baseline) of PMMA samples doped with a variable amount of Rh6G and a fixed concentration of Rh800: maximum (a), medium (b), minimum (c) and zero (d). The figures also show vertical dashed lines that indicate the red-shift of the main absorbance band as the Rh6G concentration increases.

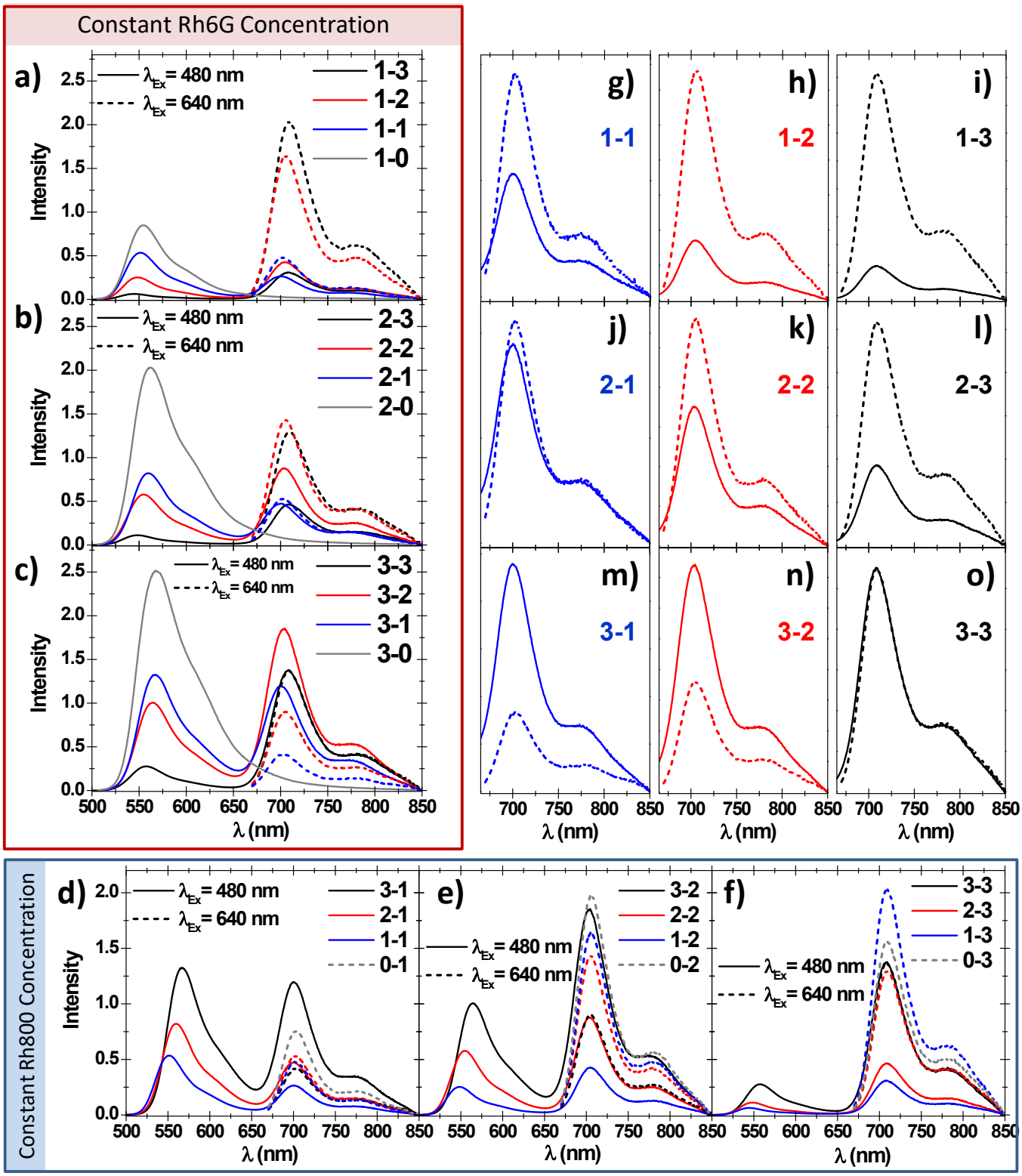

Figure S2. Fluorescence spectra using excitation light at 480 (solid line) and 640 nm(dashed line) of Rh6G-Rh800/PMMA thin films containing a fixed concentration of Rh6G (low (1), a), medium (2), b), and high (3), c)) and variable amounts of Rh800 and vice versa (d-f). g-o) Same spectra shown in Figures a-f) magnified in the Rh800 emission range, scaled to the maximum emission to compare the fluorescence intensity in the NIR and visualize the EAL behaviour.

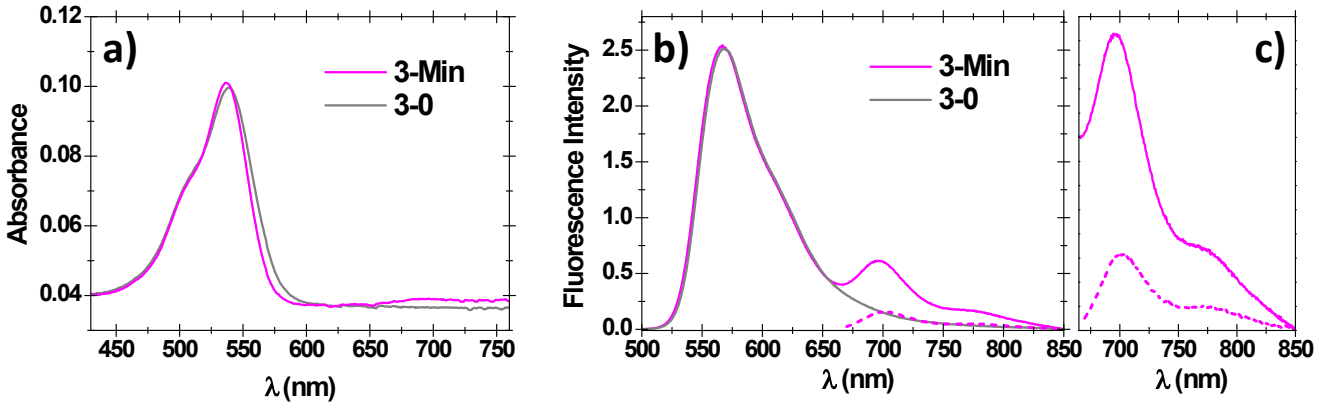

Figure S3. a) Absorbance spectra of Rh6G-Rh800/PMMA thin films containing the highest concentration of Rh6G (3) and a low concentration of Rh800 (lower than 1, 3-Min). Due to the low concentration of Rh800, the absorption bands of this molecule cannot be appreciated. b-c) Corresponding Fluorescence spectra using excitation light at 480 nm (solid line) and 640 (dashed line). The figures also show the spectra of samples without Rh800 (3-0, grey line). c) Same spectra shown in Figure b) magnified in the Rh800 emission range, scaled to the maximum emission. The contribution of the tail of the Rh6G fluorescence in the Rh800 emission range (by exciting the samples at 480 nm) was taken into account for the EAL factor calculation. Thus, the EAL factor is not significantly increased for the sample 3-Min as it can be seen in the Figure 4 c).

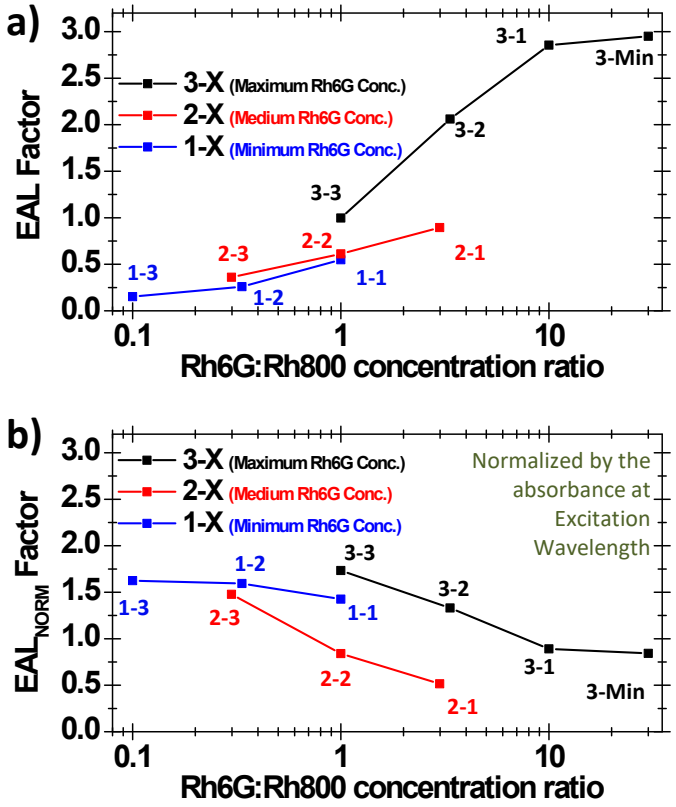

Figure S4. a) Enhanced Acceptor Luminescence (EAL) Factor the versus relative concentration C_{Rh6G}/C_{Rh800} in logarithmic scale. b) Same graph but representing the EAL factor normalised by the absorbance at the excitation wavelength:

$$EAL_{NORM} = \frac{I_{NIR}(\lambda_{EX} = 480nm) \,/\, Abs(480\ nm)}{I_{NIR}(\lambda_{EX} = 640nm) \,/\, Abs(640\ nm)}$$

Table S2. Lifetimes, pre-exponentia ... factor and the associated lifetime, respect ... or the three cases studied, Excitation/Emis ... y. The calculated average lifetimes shown ...

Rh6G - Rh800	DD: Donor Excitation 465 nm Acceptor Emission 560 nm				DA: Donor Excitation 465 nm Acceptor Emission 710 nm						AA: Donor Excitation 625 nm Acceptor Emission 560 nm			
	τ_D' (ns)	P [RA]	$\tau_{(D+DA)}$ (ns)	P [RA]	$\tau_{(D+DA)}$ (ns)	P [RA]	τ_A (ns)	P [RA]	τ_A' (ns)	P [RA]	τ_A (ns)	P [RA]	τ_A' (ns)	P [RA]
1-1	2.72	3.48E-02 [76.06 %]	0.60	4.92E-02 [23.94 %]	0.77	-3.47E-02 [-14.82 %]	3.14	6.59E-02 [114.82 %]			2.99	1.83E-02 [42.52 %]	1.99	3.72E-02 [57.48 %]
2-1	2.64	3.05E-02 [62.19 %]	1.43	3.43E-02 [37.81 %]	1.37	-4.45E-02 [-33.02 %]	2.99	8.23E-02 [133.02 %]			2.91	2.54E-02 [61.23 %]	1.49	3.13E-02 [38.77 %]
3-1	2.29	1.69E-02 [38.92 %]	0.88	6.928E-02 [61.08 %]	0.65	-4.92E-02 [-18.66 %]	2.79	7.02E-02 [115.05 %]	11.28	5.44E-04 [3.61 %]	2.51	3.311E-02 [76.10 %]	0.23	11.22E-02 [23.90 %]
1-2	1.82	1.81E-02 [37.41 %]	0.67	8.17E-02 [62.59 %]	0.43	-4.18E-02 [-13.37 %]	2.25	6.76E-02 [113.37 %]			2.13	4.10E-02 [81.96 %]	0.44	4.34E-02 [18.04 %]
2-2	1.72	2.89 [52.70 %]	0.66	6.76E-02 [47.30 %]	0.55	-5.13E-02 [-19.35 %]	2.40	7.24E-02 [119.35 %]			2.23	4.08E-02 [83.37 %]	0.49	3.68E-02 [16.63 %]
3-2	2.58	5.56E-03 [15.98 %]	0.93	8.12E-02 [84.02 %]	0.83	-4.646E-02 [-24.56 %]	2.40	7.88E-02 [121.43 %]	8.76	5.55E-04 [3.13 %]	2.33	3.75E-02 [81.23 %]	0.40	4.99E-02 [18.77 %]
1-3	0.23	2.81E-01 [95.82 %]	3.05	9.20E-04 [4.18 %]	2.63	3.19-03 [9.40 %]	1.01	0.08 [90.60 %]			1.41	2.06E-02 [38.87 %]	0.28	1.64E-01 [61.13 %]
2-3	0.19	3.5E-01 [96.22 %]	2.99	8.54E-04 [3.78 %]	3.07	1.59E-03 [5.59 %]	0.95	8.64E-02 [94.41 %]			0.80	8.57E-02 [86.12 %]	1.90	5.80E-03 [13.88 %]
3-3	2.53	9.63E-04 [3.66 %]	0.33	1.95E-01 [96.34 %]	0.27	-4.24E-02 [-11.14 %]	1.34	7.64E-02 [97.96 %]	2.94	4.69E-03 [13.18 %]	1.21	6.48E-02 [86.67 %]	2.60	4.63E-03 [13.33 %]

Rh6G	τ_{Rh6G} (ns)	P [RA]	τ_{Rh6G}' (ns)	P [RA]
1-0	3.09	4.32E-02 [78.03 %]	4.35	8.65E-03 [21.97 %]
	$<\tau_{Rh6G}(1\text{-}0)> = 3.37$ ns			
2-0	2.74	3.62E-02 [59.49 %]	3.88	1.74E-02 [40.51 %]
	$<\tau_{Rh6G}(2\text{-}0)> = 3.20$ ns			
3-0	2.15	4.71E-02 [68.98 %]	3.85	1.18E-02 [31.02 %]
	$<\tau_{Rh6G}(3\text{-}0)> = 2.68$ ns			

Rh800	τ_{Rh800} (ns)	P [RA]	τ_{Rh800}' (ns)	P [RA]
0-1	2.40	5.18E-02 [99.01 %]	1.55	8.0E-05 [0.99 %]
	$<\tau_{Rh800}(0\text{-}1)> = 2.39$ ns			
0-2	2.07	5.78E-02 [99.20 %]	12.78	7.58E-05 [0.80 %]
	$<\tau_{Rh800}(0\text{-}2)> = 2.16$ ns			
0-3	0.75	9.90E-02 [93.92 %]	2.61	1.83E-03 [6.08 %]
	$<\tau_{Rh800}(0\text{-}3)> = 0.86$ ns			

Please do not adjust margins

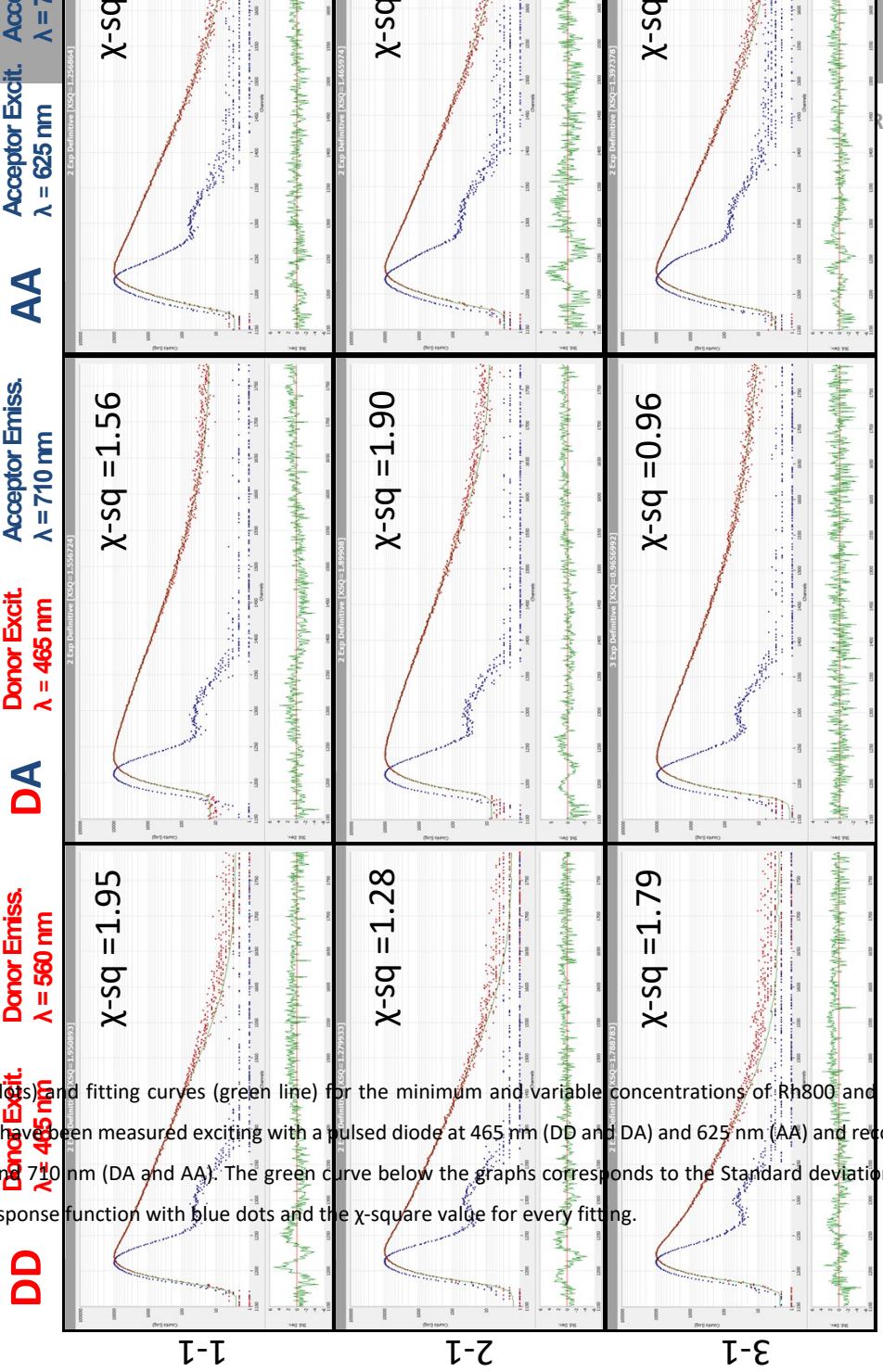

Figure S5. Fluorescent decay (red dots) and fitting curves (green line) for the minimum and variable concentrations of Rh800 and Rh6G, respectively. The time decay curves have been measured exciting with a pulsed diode at 465 nm (DD and DA) and 625 nm (AA) and recording the luminescence at 560 nm (DD) and 710 nm (DA and AA). The green curve below the graphs corresponds to the Standard deviation. The figures also show the instrument response function with blue dots and the χ-square value for every fitting.

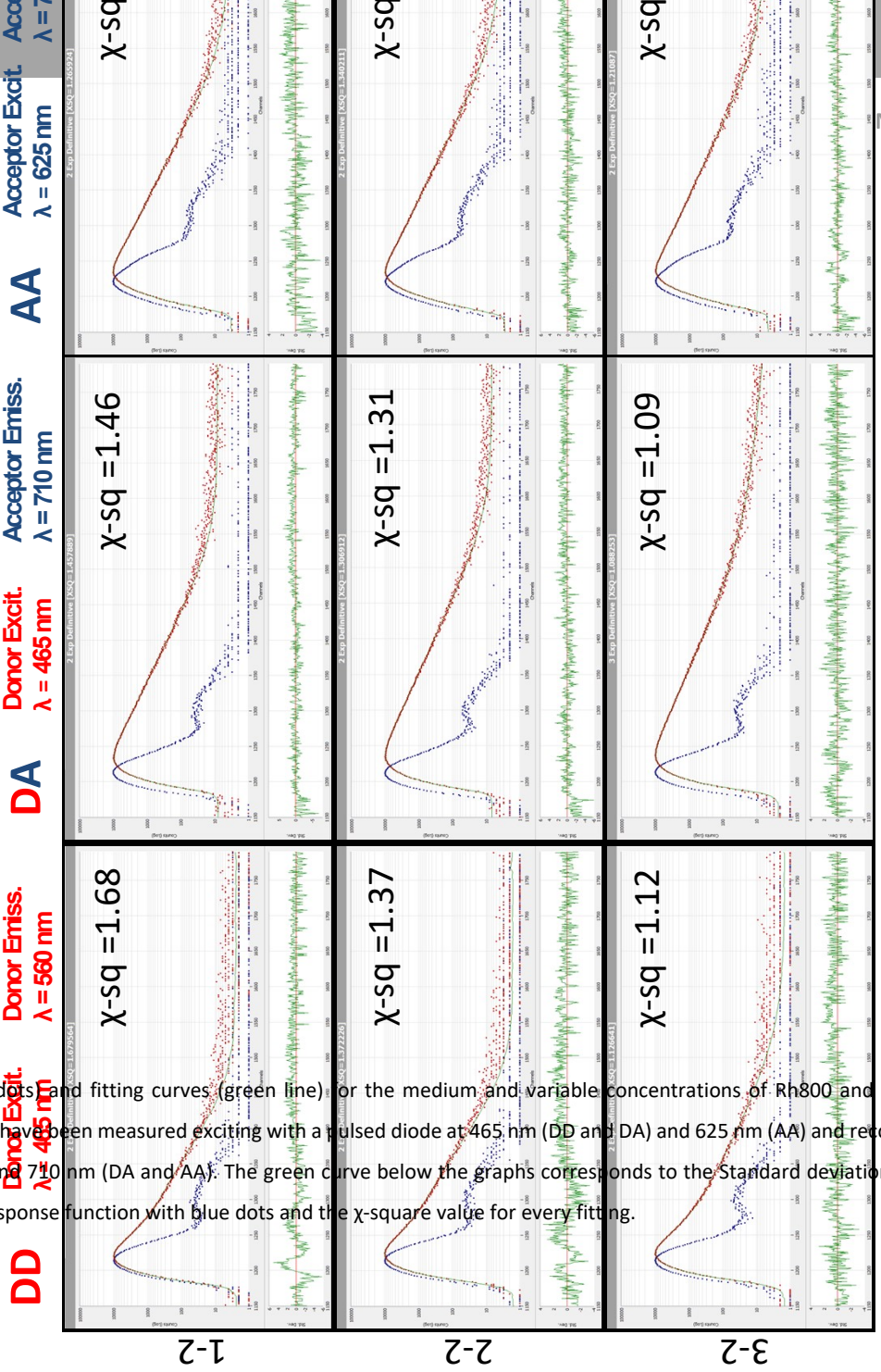

Figure S6. Fluorescent decay (red dots) and fitting curves (green line) for the medium and variable concentrations of Rh800 and Rh6G, respectively. The time decay curves have been measured exciting with a pulsed diode at 465 nm (DD and DA) and 625 nm (AA) and recording the luminescence at 560 nm (DD) and 710 nm (DA and AA). The green curve below the graphs corresponds to the Standard deviation. The figures also show the instrument response function with blue dots and the χ-square value for every fitting.

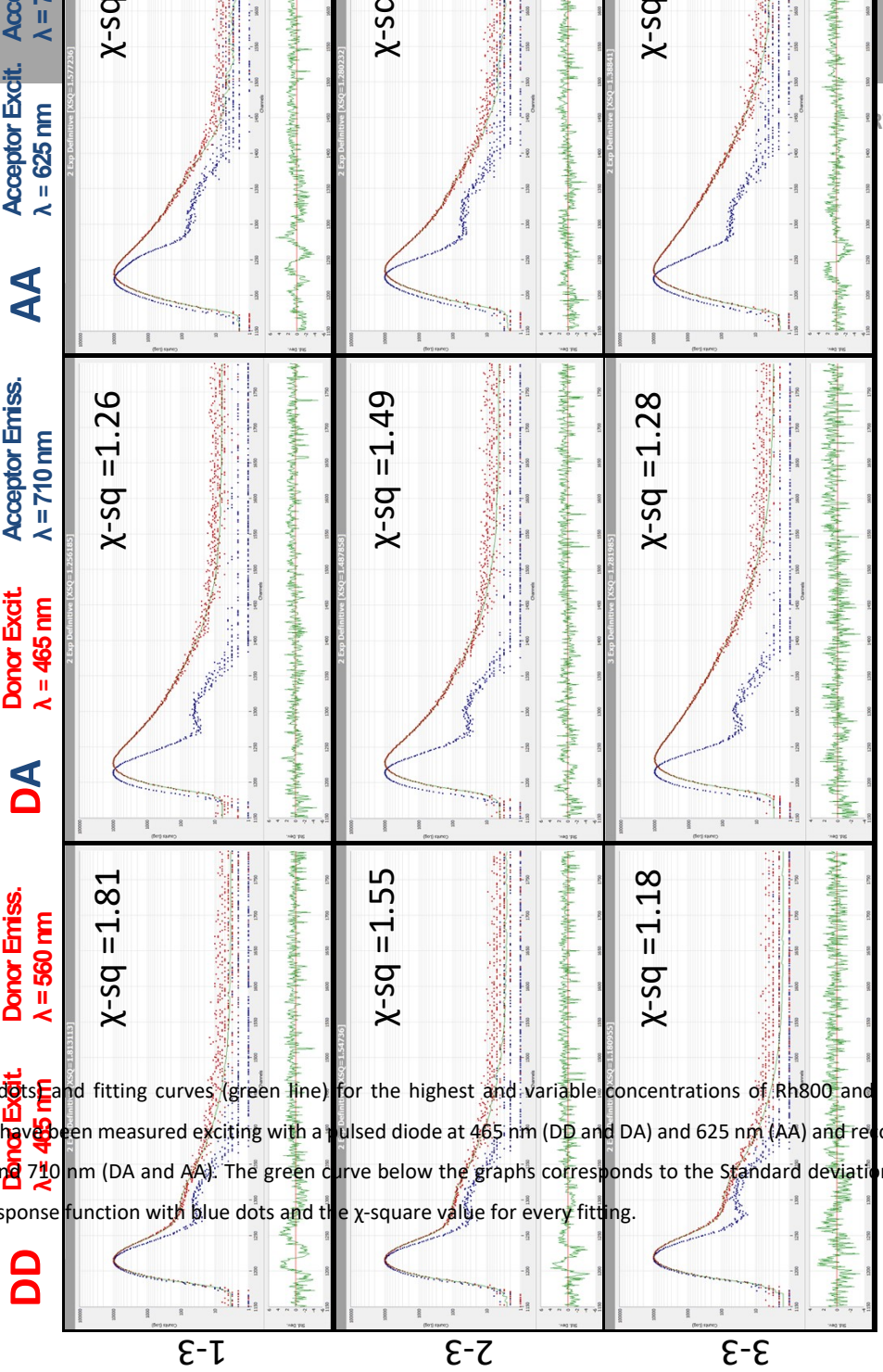

Figure S7. Fluorescent decay (red dots) and fitting curves (green line) for the highest and variable concentrations of Rh800 and Rh6G, respectively. The time decay curves have been measured exciting with a pulsed diode at 465 nm (DD and DA) and 625 nm (AA) and recording the luminescence at 560 nm (DD) and 710 nm (DA and AA). The green curve below the graphs corresponds to the Standard deviation. The figures also show the instrument response function with blue dots and the χ-square value for every fitting.